A user-friendly tool for cloud-based whole slide image segmentation, with examples from renal histopathology –**Supplemental Material**

SUPPLIMENTAL FIGURES

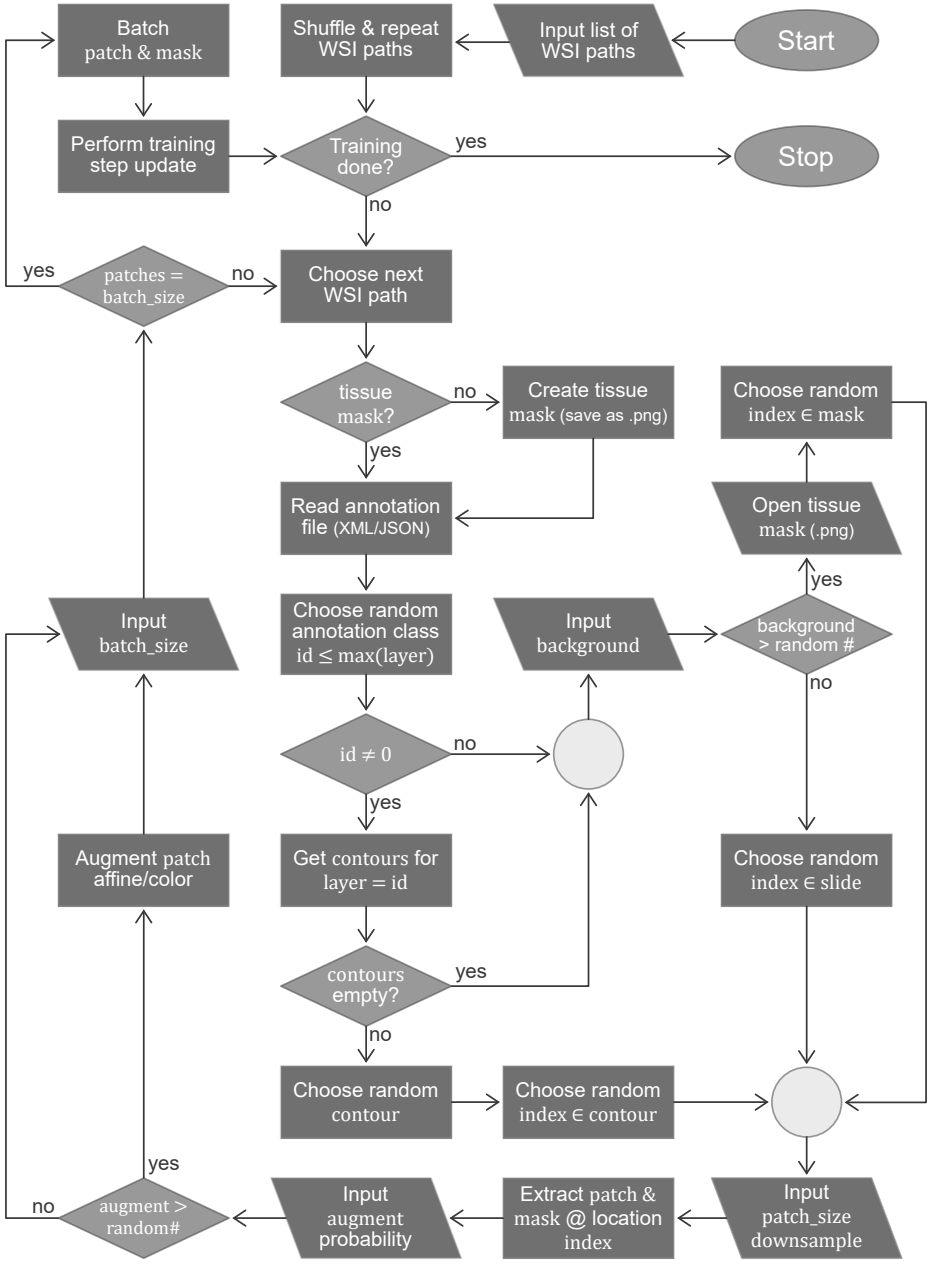

Supplemental Fig. 1 | Flowchart of the custom DeepLab WSI input pipeline.

The details of the custom input pipeline used by our modified DeepLab code to ingest WSI data during training. The *large_image* python library (https://github.com/girder/large_image/) is used to extract patches from WSIs on-the-fly. This process uses a modified version of our *HistoFetch* pipeline[1], which has been further modified to work for supervised learning tasks. For the network training, pixel locations from the image data corresponding to each data class are randomly selected by exploiting the XML or JSON annotation files. This ensures class balancing for network training by selecting appropriately sampled pixel regions for all the classes. If the background class is selected, a random location within the tissue region (which has been pre-segmented via morphological processing) is selected. During application development, we found that occasionally providing the network with non-tissue patches as background helped the batch normalization parameters to generalize, which reduced error. We therefore added a parameter defining the probability of selection of a non-tissue region, allowing patches within and outside the tissue regions to be included in the analyses. When using a trained model to segment structures (prediction on new slides), a similar pipeline is used. However, image patches to be processed are extracted deterministically from an overlapping grid pattern (excluding non-tissue regions), to ensure the entire tissue region is processed for full segmentation. This input pipeline is predominantly implemented in the following files in the DeepLab codebase available via github: /datasets/wsi_data_generator.py and /utils/wsi_dataset_util_large_image.py

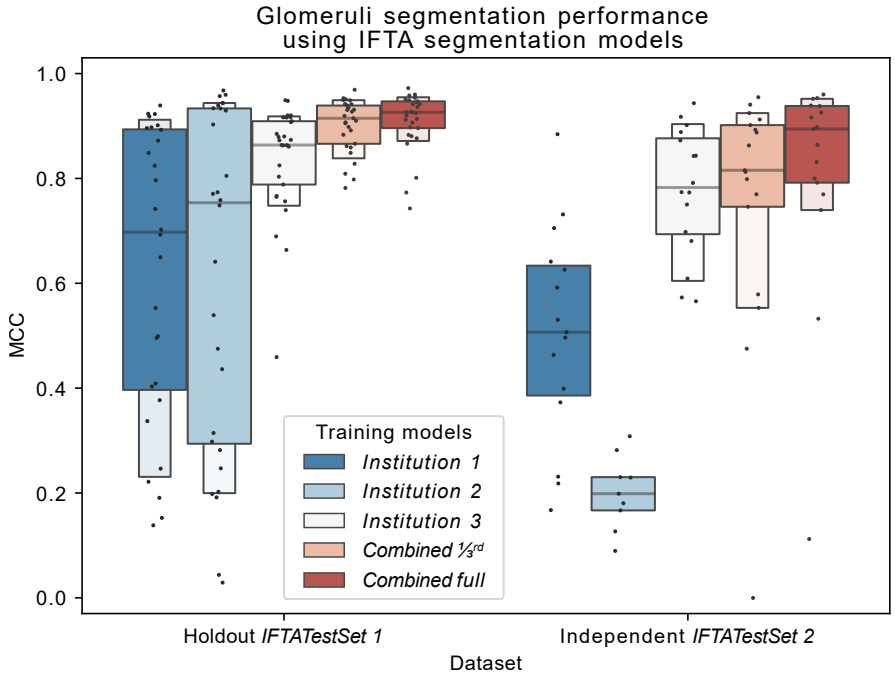

***Supplemental Fig. 2* |** Glomeruli segmentation performance using IFTA segmentation models.

The glomerular segmentation performance using the five models trained for segmenting IFTA and glomeruli (see *IFTA SEGMENTATION – adaptability* under *RESULTS* and ***Fig. 4***). The performance is quantified on the *IFTATestSet 1* with 29 holdout renal tissue WSIs, and the independent test set *IFTATestSet 2* with 17 renal tissue WSIs and annotation ground-truth originated from an institution independent of the training dataset and *IFTATestSet 1*. We observe the same trend in performance as IFTA segmentation as shown in ***Fig. 4***. Namely, the *Combined full* model delivers the best performance, while the *Combined 1/3rd* model performs better than any of the models trained on a single institution data alone.

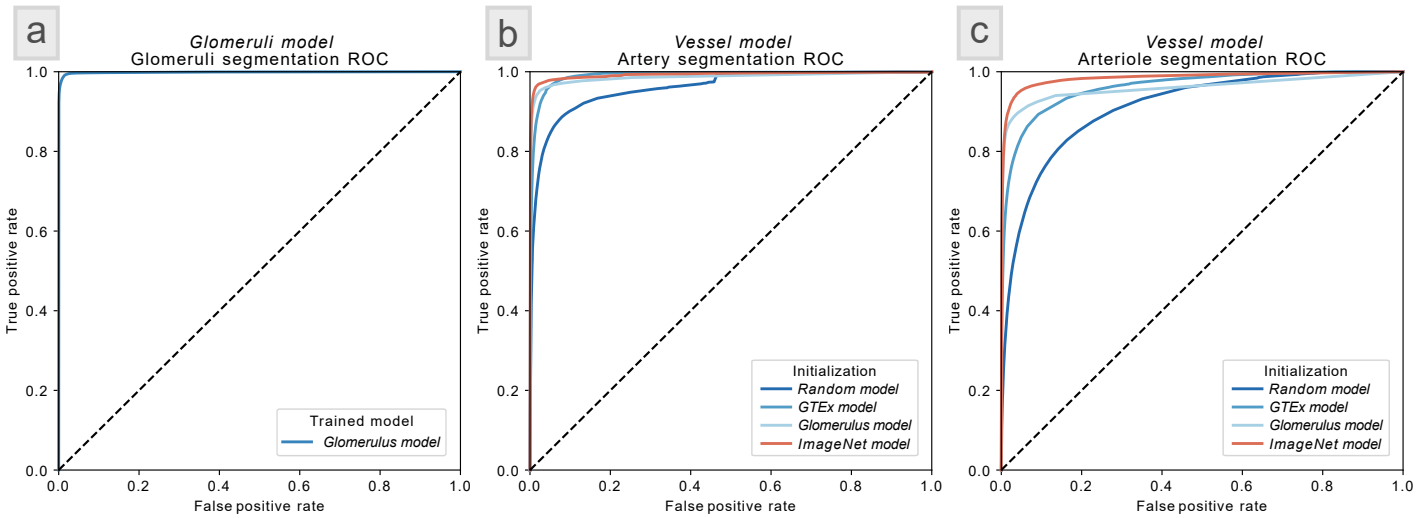

Supplemental Fig. 3 **|** ROC performance for glomeruli and vessel segmentation.

Panel [a] shows the ROC performance for glomerular segmentation on *GlomTestSet 1* with 100 holdout renal tissue WSIs using *glomerular model* (see *GLOMERULI SEGMENTATION – scalability* in *RESULTS* and ***Fig. 2***). **[b]** shows the ROC performance for artery segmentation on the holdout dataset *VessTestSet* with 58 renal tissue WSIs using the four initialization strategies for vessel segmentation (see *VESSEL SEGMENTATION – adaptability* in *RESULTS* and ***Fig. 3***). **[c]** shows the ROC performance for arteriole segmentation on the same holdout dataset with same initialization strategies as used in **[b]**.

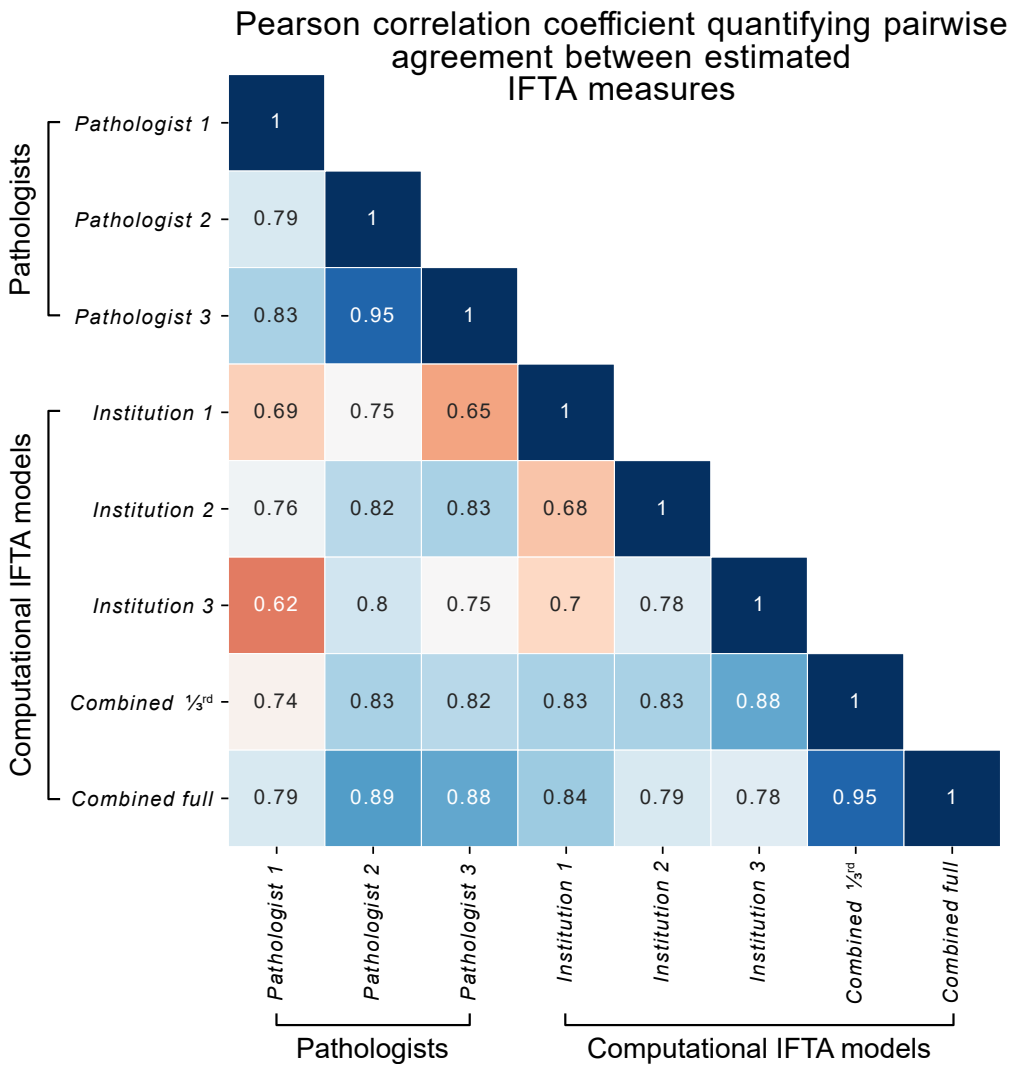

Supplemental Fig. 4 **|** Correlation of percent IFTA estimation between methods.

Pearson correlation coefficient quantifying pairwise agreement between computationally and manually estimated IFTA measures for 26 CKD renal tissue WSIs from Kidney Precision Medicine Project (KPMP) cohort data, *KPMPTestSet*. The full confusion matrix of correlations of computationally estimated and visually manually estimated percent IFTA for the KPMP test cohort. Pairwise correlations were measured for each pair of the three KPMP pathologists and the five computational models trained for IFTA segmentation (see *IFTA SEGMENTATION – adaptability* under *RESULTS*). This result is an extension of ***Fig. 4c***. Pearson correlation coefficients with p-value < 0.05 are shown.

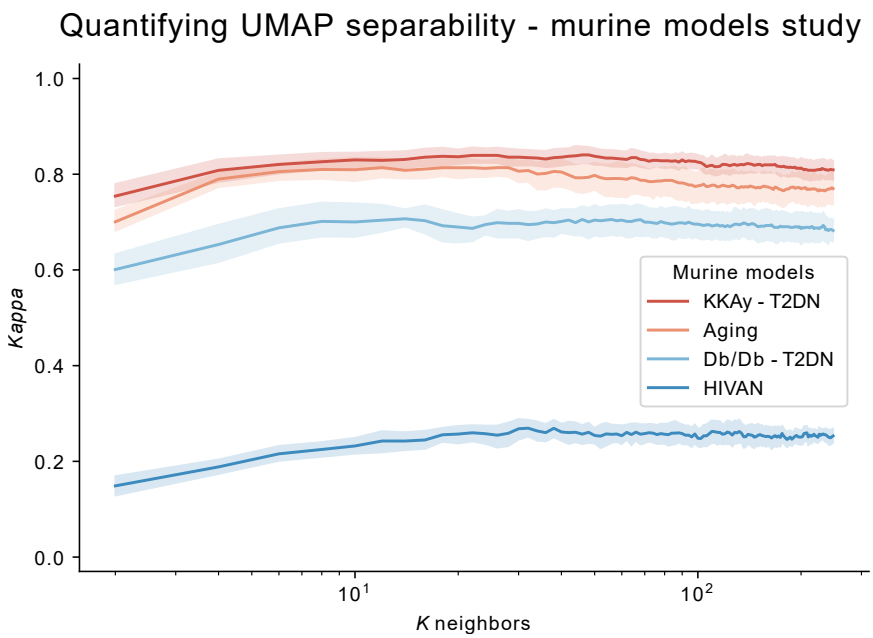

Supplemental Fig. 5 **|** Quantifying UMAP separability for the murine model studies.

K-nearest neighbors (KNN) classifier performance plotting the *Cohen's Kappa* measure as a function of *K* neighbors for classifying the unsupervised UMAP features with respect to disease vs control status for the murine kidney disease models (see ***Fig. 5***). This analysis was done using 10-fold cross validation using a similar method as formalized in a previous work[2].

TABLE OF ABBREVIATIONS

Supplementary Table 1 | Features measured on each glomerulus.

AUC	Area under the curve
CKD	Chronic kidney disease
CNN	Convolutional neural network
DSA	Digital slide archive
eGFR	Estimated glomerular filtration rate
FSGS	Focal segmental glomerulosclerosis
GPU	G**raphics processing unit**
GTEx	Genotype-tissue expression
H-AI-L	Human – Artificial Intelligence – Loop
H&E	Hematoxylin and eosin (stain)
HIVAN	HIV-associated nephropathy
IFTA	Interstitial fibrosis and tubular atrophy
IoU	Intersection over Union (Jaccard index)
JSON	JavaScript object notation
KD	Knockdown
KPMP	Kidney precision medicine project
MCC	Matthews correlation coefficient
PAS	Periodic acid–Schiff (stain)
PNG	Portable network graphics
RAM	R**andom access memory**
ROC	Receiver operating characteristic
STZ	Streptozotocin
T2DN	Type 2 diabetic nephropathy
uACR	Albumin to creatinine ratio
UMAP	Uniform manifold approximation and projection
uPCR	Urinary protein to creatinine ratio
VRAM	V**ideo RAM**
WSI	Whole slide image
XML	Extensible markup language

GLOMERULAR FEATURES

Supplementary Table 2 | Features measured on each glomerulus.

Note that each segmented glomerulus is further computationally sub-compartmentalized for PAS+ area, nuclei, and luminal white spaces, and the features are subsequently quantified from these sub-compartments using a method as discussed in our previous work3. In the list below C represents the color features, D the distance features, M the morphological features, T the textural features, and PAS+ the periodic acid-Schiff positive features.

Index	Feature Name	Type
1	Mean of red values in PAS+ regions	C
2	Mean of green values in PAS+ regions	C
3	Mean of blue values in PAS+ regions	C
4	Standard deviation of red values in PAS+ regions	C
5	Standard deviation of green values in PAS+ regions	C
6	Standard deviation of blue values in PAS+ regions	C
7	Mean of red values in luminal regions	C
8	Mean of green values in luminal regions	C
9	Mean of blue values in luminal regions	C
10	Standard deviation of red values in luminal regions	C
11	Standard deviation of green values in luminal regions	C
12	Standard deviation of blue values in luminal regions	C
13	Mean of red values in nuclear regions	C
14	Mean of green values in nuclear regions	C
15	Mean of blue values in nuclear regions	C
16	Standard deviation of red values in nuclear regions	C
17	Standard deviation of green values in nuclear regions	C
18	Standard deviation of blue values in nuclear regions	C
19	Mean distance of luminal object centroids from glomerular centroid	D
20	Mean of mean distances of luminal object centroids from glomerular boundary	D
21	Mean of maximum distances of luminal object centroids from glomerular boundary	D
22	Mean of minimum distances of luminal object centroids from glomerular boundary	D
23	Mean of mean distances of luminal object centroids from themselves	D
24	Mean of maximum distances of luminal object centroids from themselves	D
25	Mean of minimum distances of luminal object centroids from themselves	D
26	Mean distance of PAS+ object centroids from glomerular centroid	D
27	Mean of mean distances of PAS+ object centroids from glomerular boundary	D
28	Mean of maximum distances of PAS+ object centroids from glomerular boundary	D
29	Mean of minimum distances of PAS+ object centroids from glomerular boundary	D
30	Mean of mean distances of PAS+ object centroids from themselves	D
31	Mean of maximum distances of PAS+ object centroids from themselves	D
32	Mean of minimum distances of PAS+ object centroids from themselves	D
33	Mean distance of nuclear object centroids from glomerular centroid	D
34	Mean of mean distances of nuclear object centroids from glomerular boundary	D
35	Mean of maximum distances of nuclear object centroids from glomerular boundary	D
36	Mean of minimum distances of nuclear object centroids from glomerular boundary	D
37	Mean of mean distances of nuclear object centroids from themselves	D
38	Mean of maximum distances of nuclear object centroids from themselves	D
39	Mean of minimum distances of nuclear object centroids from themselves	D
40	Average luminal object solidity	M
41	Average PAS+ region contained in luminal object boundaries	M

42	Average nuclear region contained in luminal object boundaries	M
43	Sum total luminal objects' areas	M
44	Mean of luminal objects' areas	M
45	Median of luminal objects' areas	M
46	Average PAS+ object solidity	M
47	Average lumina region contained in PAS+ object boundaries	M
48	Average nuclear region contained in PAS+ object boundaries	M
49	Sum total PAS+ objects' areas	M
50	Mean of PAS+ objects' areas	M
51	Median of PAS+ objects' areas	M
52	Mean ratio of PAS+ pixels lying just outside nuclear perimeter to length of perimeter	M
53	Mean ratio of luminal pixels lying just outside nuclear perimeter to length of perimeter	M
54	Mean nuclear perimeter pixel count	M
55	Sum total nuclear area	M
56	Mean nuclear areas	M
57	Mode nuclear areas	M
58	Total glomerular area	M
59	Total PAS+ object number	M
60	Total luminal object number	M
61	Total nucleus number	M
62	Sum of PAS+ distance transform values 0µm < d ≤ 2.5µm	M
63	Sum of PAS+ distance transform values 2.5µm < d ≤ 5µm	M
64	Sum of PAS+ distance transform values 5µm < d ≤ 250µm	M
65	Maximum PAS+ distance transform value 2.5µm < d ≤ 5µm	M
66	Number of connected objects with PAS+ distance transform value 0µm < d ≤ 2.5µm	M
67	Number of connected objects with PAS+ distance transform value 2.5 µm < d ≤ 5µm	M
68	Mean of PAS+ distance transform values 0µm < d ≤ 2.5µm	M
69	Mean of PAS+ distance transform values 2.5µm < d ≤ 5µm	M
70	Median of PAS+ distance transform values 0µm < d ≤ 2.5µm	M
71	Median of PAS+ distance transform values 2.5µm < d ≤ 5µm	M
72	Mean area of objects with PAS+ distance transform value 0µm < d ≤ 2.5µm	M
73	Median area of objects with PAS+ distance transform value 0µm < d ≤ 2.5µm	M
74	Maximum area of objects with PAS+ distance transform value 0µm < d ≤ 2.5µm	M
75	Mean area of objects with PAS+ distance transform value 2.5µm < d ≤ 5µm	M
76	Median area of objects with PAS+ distance transform value 2.5µm < d ≤ 5µm	M
77	Count of pixels with PAS+ distance transform value 0.25µm < d ≤ 0.75µm	M
78	Count of pixels with PAS+ distance transform value 0.75µm < d ≤ 1.25µm	M
79	Count of pixels with PAS+ distance transform value 1.25µm < d ≤ 1.75µm	M
80	Count of pixels with PAS+ distance transform value 1.75µm < d ≤ 2.25µm	M
81	Count of pixels with PAS+ distance transform value 2.25µm < d ≤ 2.75µm	M
82	Count of pixels with PAS+ distance transform value 2.75µm < d ≤ 3.25µm	M
83	Count of pixels with PAS+ distance transform value 3.25µm < d ≤ 3.75µm	M
84	Count of pixels with PAS+ distance transform value 3.75µm < d ≤ 4.25µm	M
85	Count of pixels with PAS+ distance transform value 4.25µm < d ≤ 4.75µm	M
86	Count of pixels with PAS+ distance transform value 4.75µm < d ≤ 5.25µm	M
87	Count of pixels with PAS+ distance transform value 5.25µm < d ≤ 5.75µm	M
88	Count of pixels with PAS+ distance transform value 5.75µm < d ≤ 6.25µm	M

89	Count of pixels with PAS+ distance transform value 6.25µm < d ≤ 6.75µm	M
90	Count of pixels with PAS+ distance transform value 6.75µm < d ≤ 7.25µm	M
91	Count of pixels with PAS+ distance transform value 7.25µm < d ≤ 7.75µm	M
92	Count of pixels with PAS+ distance transform value 7.75µm < d ≤ 8.25µm	M
93	Count of pixels with PAS+ distance transform value 8.25µm < d ≤ 8.75µm	M
94	Count of pixels with PAS+ distance transform value 8.75µm < d ≤ 9.25µm	M
95	Count of pixels with PAS+ distance transform value 9.25µm < d ≤ 9.75µm	M
96	Count of pixels with PAS+ distance transform value 9.75µm < d ≤ 10.25µm	M
97	Count of pixels with PAS+ distance transform value 10.25µm < d ≤ 10.75µm	M
98	Count of pixels with PAS+ distance transform value 10.75µm < d ≤ 11.25µm	M
99	Count of pixels with PAS+ distance transform value 11.25µm < d ≤ 11.75µm	M
100	Count of pixels with PAS+ distance transform value 11.75µm < d ≤ 12.25µm	M
101	Count of pixels with PAS+ distance transform value 12.25µm < d ≤ 12.75µm	M
102	Count of pixels with PAS+ distance transform value 12.75µm < d ≤ 13.25µm	M
103	Count of pixels with PAS+ distance transform value 13.25µm < d ≤ 13.75µm	M
104	Count of pixels with PAS+ distance transform value 13.75µm < d ≤ 14.25µm	M
105	Count of pixels with PAS+ distance transform value 14.25µm < d ≤ 14.75µm	M
106	Count of pixels with PAS+ distance transform value 14.75µm < d ≤ 15.25µm	M
107	Count of pixels with PAS+ distance transform value 15.25µm < d ≤ 15.75µm	M
108	Count of pixels with PAS+ distance transform value 15.75µm < d ≤ 16.25µm	M
109	Count of pixels with PAS+ distance transform value 16.25µm < d ≤ 16.75µm	M
110	Count of pixels with PAS+ distance transform value 16.75µm < d ≤ 17.25µm	M
111	Count of pixels with PAS+ distance transform value 17.25µm < d ≤ 17.75µm	M
112	Count of pixels with PAS+ distance transform value 17.75µm < d ≤ 18.25µm	M
113	Count of pixels with PAS+ distance transform value 18.25µm < d ≤ 18.75µm	M
114	Count of pixels with PAS+ distance transform value 18.75µm < d ≤ 19.25µm	M
115	Count of pixels with PAS+ distance transform value 19.25µm < d ≤ 19.75µm	M
116	Count of pixels with PAS+ distance transform value 19.75µm < d ≤ 500µm	M
117	Count of pixels with luminal distance transform value 0.25µm < d ≤ 0.5µm	M
118	Count of pixels with luminal distance transform value 0.5µm < d ≤ 0.75µm	M
119	Count of pixels with luminal distance transform value 0.75µm < d ≤ 1µm	M
120	Count of pixels with luminal distance transform value 1µm < d ≤ 1.25µm	M
121	Count of pixels with luminal distance transform value 1.25µm < d ≤ 1.5µm	M
122	Count of pixels with luminal distance transform value 1.5µm < d ≤ 1.75µm	M
123	Count of pixels with luminal distance transform value 1.75µm < d ≤ 2µm	M
124	Count of pixels with luminal distance transform value 2µm < d ≤ 2.25µm	M
125	Count of pixels with luminal distance transform value 2.25µm < d ≤ 2.5µm	M
126	Count of pixels with luminal distance transform value 2.5µm < d ≤ 2.75µm	M
127	Count of pixels with luminal distance transform value 2.75µm < d ≤ 3µm	M
128	Count of pixels with luminal distance transform value 3µm < d ≤ 3.25µm	M
129	Count of pixels with luminal distance transform value 3.25µm < d ≤ 3.5µm	M
130	Count of pixels with luminal distance transform value 3.5µm < d ≤ 3.75µm	M
131	Count of pixels with luminal distance transform value 3.75µm < d ≤ 4µm	M
132	Count of pixels with luminal distance transform value 4µm < d ≤ 4.25µm	M
133	Count of pixels with luminal distance transform value 4.25µm < d ≤ 4.5µm	M
134	Count of pixels with luminal distance transform value 4.5µm < d ≤ 4.75µm	M
135	Count of pixels with luminal distance transform value 4.75µm < d ≤ 5µm	M
136	Count of pixels with luminal distance transform value 5µm < d ≤ 5.25µm	M

137	Count of pixels with luminal distance transform value 5.25µm < d ≤ 5.5µm	M
138	Count of pixels with luminal distance transform value 5.5µm < d ≤ 5.75µm	M
139	Count of pixels with luminal distance transform value 5.75µm < d ≤ 6µm	M
140	Count of pixels with luminal distance transform value 6µm < d ≤ 6.25µm	M
141	Count of pixels with luminal distance transform value 6.25µm < d ≤ 6.5µm	M
142	Count of pixels with luminal distance transform value 6.5µm < d ≤ 6.75µm	M
143	Count of pixels with luminal distance transform value 6.75µm < d ≤ 7µm	M
144	Count of pixels with luminal distance transform value 7µm < d ≤ 7.25µm	M
145	Count of pixels with luminal distance transform value 7.25µm < d ≤ 7.5µm	M
146	Count of pixels with luminal distance transform value 7.5µm < d ≤ 7.75µm	M
147	Count of pixels with luminal distance transform value 7.75µm < d ≤ 8µm	M
148	Count of pixels with luminal distance transform value 8µm < d ≤ 8.25µm	M
149	Count of pixels with luminal distance transform value 8.25µm < d ≤ 8.5µm	M
150	Count of pixels with luminal distance transform value 8.5µm < d ≤ 8.75µm	M
151	Count of pixels with luminal distance transform value 8.75µm < d ≤ 9µm	M
152	Count of pixels with luminal distance transform value 9µm < d ≤ 9.25µm	M
153	Count of pixels with luminal distance transform value 9.25µm < d ≤ 9.5µm	M
154	Count of pixels with luminal distance transform value 9.5µm < d ≤ 9.75µm	M
155	Count of pixels with luminal distance transform value 9.75µm < d ≤ 10µm	M
156	Count of pixels with luminal distance transform value 10µm < d ≤ 10.25µm	M
157	Count of pixels with luminal distance transform value 10.25µm < d ≤ 10.5µm	M
158	Count of pixels with luminal distance transform value 10.5µm < d ≤ 10.75µm	M
159	Count of pixels with luminal distance transform value 10.75µm < d ≤ 11µm	M
160	Count of pixels with luminal distance transform value 11µm < d ≤ 11.25µm	M
161	Count of pixels with luminal distance transform value 11.25µm < d ≤ 11.5µm	M
162	Count of pixels with luminal distance transform value 11.5µm < d ≤ 11.75µm	M
163	Count of pixels with luminal distance transform value 11.75µm < d ≤ 12µm	M
164	Count of pixels with luminal distance transform value 12µm < d ≤ 12.25µm	M
165	Count of pixels with luminal distance transform value 12.25µm < d ≤ 12.5µm	M
166	Count of pixels with luminal distance transform value 12.5µm < d ≤ 12.75µm	M
167	Count of pixels with luminal distance transform value 12.75µm < d ≤ 13µm	M
168	Count of pixels with luminal distance transform value 13µm < d ≤ 13.25µm	M
169	Count of pixels with luminal distance transform value 13.25µm < d ≤ 13.5µm	M
170	Count of pixels with luminal distance transform value 13.5µm < d ≤ 13.75µm	M
171	Count of pixels with luminal distance transform value 13.75µm < d ≤ 14µm	M
172	Count of pixels with luminal distance transform value 14µm < d ≤ 14.25µm	M
173	Count of pixels with luminal distance transform value 14.25µm < d ≤ 14.5µm	M
174	Count of pixels with luminal distance transform value 14.5µm < d ≤ 14.75µm	M
175	Count of pixels with luminal distance transform value 14.75µm < d ≤ 15µm	M
176	Count of pixels with luminal distance transform value 15µm < d ≤ 500µm	M
177	Count of pixels with nuclear distance transform value 0.25µm < d ≤ 0.5µm	M
178	Count of pixels with nuclear distance transform value 0.5µm < d ≤ 0.75µm	M
179	Count of pixels with nuclear distance transform value 0.75µm < d ≤ 1µm	M
180	Count of pixels with nuclear distance transform value 1µm < d ≤ 1.25µm	M
181	Count of pixels with nuclear distance transform value 1.25µm < d ≤ 1.5µm	M
182	Count of pixels with nuclear distance transform value 1.5µm < d ≤ 1.75µm	M
183	Count of pixels with nuclear distance transform value 1.75µm < d ≤ 2µm	M
184	Count of pixels with nuclear distance transform value 2µm < d ≤ 2.25µm	M

185	Count of pixels with nuclear distance transform value 2.25µm < d ≤ 2.5µm	M
186	Count of pixels with nuclear distance transform value 2.5µm < d ≤ 2.75µm	M
187	Count of pixels with nuclear distance transform value 2.75µm < d ≤ 3µm	M
188	Count of pixels with nuclear distance transform value 3µm < d ≤ 3.25µm	M
189	Count of pixels with nuclear distance transform value 3.25µm < d ≤ 3.5µm	M
190	Count of pixels with nuclear distance transform value 3.5µm < d ≤ 3.75µm	M
191	Count of pixels with nuclear distance transform value 3.75µm < d ≤ 4µm	M
192	Count of pixels with nuclear distance transform value 4µm < d ≤ 4.25µm	M
193	Count of pixels with nuclear distance transform value 4.25µm < d ≤ 4.5µm	M
194	Count of pixels with nuclear distance transform value 4.5µm < d ≤ 4.75µm	M
195	Count of pixels with nuclear distance transform value 4.75µm < d ≤ 5µm	M
196	Count of pixels with nuclear distance transform value 5µm < d ≤ 500µm	M
197	Count of pixels with glomerular distance transform value 0.5µm < d ≤ 6.75µm	M
198	Count of pixels with glomerular distance transform value 6.75µm < d ≤ 13µm	M
199	Count of pixels with glomerular distance transform value 13µm < d ≤ 19.25µm	M
200	Count of pixels with glomerular distance transform value 19.25µm < d ≤ 25.5µm	M
201	Count of pixels with glomerular distance transform value 25.5µm < d ≤ 31.75µm	M
202	Count of pixels with glomerular distance transform value 31.75µm < d ≤ 38µm	M
203	Count of pixels with glomerular distance transform value 38µm < d ≤ 44.25µm	M
204	Count of pixels with glomerular distance transform value 44.25µm < d ≤ 50.5µm	M
205	Count of pixels with glomerular distance transform value 50.5µm < d ≤ 56.75µm	M
206	Count of pixels with glomerular distance transform value 56.75µm < d ≤ 63µm	M
207	Count of pixels with glomerular distance transform value 63µm < d ≤ 69.25µm	M
208	Count of pixels with glomerular distance transform value 69.25µm < d ≤ 75.5µm	M
209	Count of pixels with glomerular distance transform value 75.5µm < d ≤ 81.75µm	M
210	Count of pixels with glomerular distance transform value 81.75µm < d ≤ 88µm	M
211	Count of pixels with glomerular distance transform value 88µm < d ≤ 94.25µm	M
212	Count of pixels with glomerular distance transform value 94.25µm < d ≤ 100.5µm	M
213	Count of pixels with glomerular distance transform value 100.5µm < d ≤ 106.75µm	M
214	Count of pixels with glomerular distance transform value 106.75µm < d ≤ 113µm	M
215	Count of pixels with glomerular distance transform value 113µm < d ≤ 119.25µm	M
216	Count of pixels with glomerular distance transform value 119.25µm < d ≤ 125.5µm	M
217	Count of pixels with glomerular distance transform value 125.5µm < d ≤ 131.75µm	M
218	Count of pixels with glomerular distance transform value 131.75µm < d ≤ 138µm	M
219	Count of pixels with glomerular distance transform value 138µm < d ≤ 144.25µm	M
220	Count of pixels with glomerular distance transform value 144.25µm < d ≤ 5000µm	M
221	Number nuclear pixels contained radius 0µm < R ≤ 25µm	M
222	Number nuclear pixels contained radius 25µm < R ≤ 50µm	M
223	Number nuclear pixels contained radius 50µm < R ≤ 75µm	M
224	Number nuclear pixels contained radius 75µm < R ≤ 100µm	M
225	Number nuclear pixels contained radius 100µm < R ≤ 125µm	M
226	Number nuclear pixels contained radius 125µm < R ≤ 150µm	M
227	Number nuclear pixels contained radius 150µm < R ≤ 175µm	M
228	Number nuclear pixels contained radius 175µm < R ≤ 200µm	M
229	Number nuclear pixels contained radius 200µm < R ≤ 225µm	M
230	Number nuclear pixels contained radius 225µm < R ≤ 250µm	M
231	Number nuclear pixels contained radius 250µm < R ≤ 325µm	M
232	Number luminal pixels contained radius 0µm < R ≤ 25µm	M

233	Number luminal pixels contained radius 25µm < R ≤ 50µm	M
234	Number luminal pixels contained radius 50µm < R ≤ 75µm	M
235	Number luminal pixels contained radius 75µm < R ≤ 100µm	M
236	Number luminal pixels contained radius 100µm < R ≤ 125µm	M
237	Number luminal pixels contained radius 125µm < R ≤ 150µm	M
238	Number luminal pixels contained radius 150µm < R ≤ 175µm	M
239	Number luminal pixels contained radius 175µm < R ≤ 200µm	M
240	Number luminal pixels contained radius 200µm < R ≤ 225µm	M
241	Number luminal pixels contained radius 225µm < R ≤ 250µm	M
242	Number luminal pixels contained radius 250µm < R ≤ 325µm	M
243	Number PAS+ pixels contained radius 0µm < R ≤ 25µm	M
244	Number PAS+ pixels contained radius 25µm < R ≤ 50µm	M
245	Number PAS+ pixels contained radius 50µm < R ≤ 75µm	M
246	Number PAS+ pixels contained radius 75µm < R ≤ 100µm	M
247	Number PAS+ pixels contained radius 100µm < R ≤ 125µm	M
248	Number PAS+ pixels contained radius 125µm < R ≤ 150µm	M
249	Number PAS+ pixels contained radius 150µm < R ≤ 175µm	M
250	Number PAS+ pixels contained radius 175µm < R ≤ 200µm	M
251	Number PAS+ pixels contained radius 200µm < R ≤ 225µm	M
252	Number PAS+ pixels contained radius 225µm < R ≤ 250µm	M
253	Number PAS+ pixels contained radius 250µm < R ≤ 325µm	M
254	Number nuclear pixels contained between theta -180 < R ≤ -162	M
255	Number nuclear pixels contained between theta -162 < R ≤ -144	M
256	Number nuclear pixels contained between theta -144 < R ≤ -126	M
257	Number nuclear pixels contained between theta -126 < R ≤ -108	M
258	Number nuclear pixels contained between theta -108 < R ≤ -90	M
259	Number nuclear pixels contained between theta -90 < R ≤ -72	M
260	Number nuclear pixels contained between theta -72 < R ≤ -54	M
261	Number nuclear pixels contained between theta -54 < R ≤ -36	M
262	Number nuclear pixels contained between theta -36 < R ≤ -18	M
263	Number nuclear pixels contained between theta -18 < R ≤ 0	M
264	Number nuclear pixels contained between theta 0 < R ≤ 18	M
265	Number nuclear pixels contained between theta 18 < R ≤ 36	M
266	Number nuclear pixels contained between theta 36 < R ≤ 54	M
267	Number nuclear pixels contained between theta 54 < R ≤ 72	M
268	Number nuclear pixels contained between theta 72 < R ≤ 90	M
269	Number nuclear pixels contained between theta 90 < R ≤ 108	M
270	Number nuclear pixels contained between theta 108 < R ≤ 126	M
271	Number nuclear pixels contained between theta 126 < R ≤ 144	M
272	Number nuclear pixels contained between theta 144 < R ≤ 162	M
273	Number nuclear pixels contained between theta 162 < R ≤ 180	M
274	0.1 quantile of nuclear pixels from the boundary line	M
275	0.2 quantile of nuclear pixels from the boundary line	M
276	0.3 quantile of nuclear pixels from the boundary line	M
277	0.4 quantile of nuclear pixels from the boundary line	M
278	0.5 quantile of nuclear pixels from the boundary line	M
279	0.6 quantile of nuclear pixels from the boundary line	M
280	0.7 quantile of nuclear pixels from the boundary line	M

281	0.8 quantile of nuclear pixels from the boundary line	M
282	0.9 quantile of nuclear pixels from the boundary line	M
283	1 quantile of nuclear pixels from the boundary line	M
284	0.1 quantile of luminal pixels from the boundary line	M
285	0.2 quantile of luminal pixels from the boundary line	M
286	0.3 quantile of luminal pixels from the boundary line	M
287	0.4 quantile of luminal pixels from the boundary line	M
288	0.5 quantile of luminal pixels from the boundary line	M
289	0.6 quantile of luminal pixels from the boundary line	M
290	0.7 quantile of luminal pixels from the boundary line	M
291	0.8 quantile of luminal pixels from the boundary line	M
292	0.9 quantile of luminal pixels from the boundary line	M
293	1 quantile of luminal pixels from the boundary line	M
294	0.1 quantile of mesangial pixels from the boundary line	M
295	0.2 quantile of mesangial pixels from the boundary line	M
296	0.3 quantile of mesangial pixels from the boundary line	M
297	0.4 quantile of mesangial pixels from the boundary line	M
298	0.5 quantile of mesangial pixels from the boundary line	M
299	0.6 quantile of mesangial pixels from the boundary line	M
300	0.7 quantile of mesangial pixels from the boundary line	M
301	0.8 quantile of mesangial pixels from the boundary line	M
302	0.9 quantile of mesangial pixels from the boundary line	M
303	1 quantile of mesangial pixels from the boundary line	M
304	Luminal textural contrast	T
305	Luminal textural correlation	T
306	Luminal textural energy	T
307	Luminal textural homogeneity	T
308	PAS+ textural contrast	T
309	PAS+ textural correlation	T
310	PAS+ textural energy	T
311	PAS+ textural homogeneity	T
312	Nuclear textural contrast	T
313	Nuclear textural correlation	T
314	Nuclear textural energy	T
315	Nuclear textural homogeneity	T

SUPPLEMENTAL REFERENCES

1 Lutnick, B., Krishna, L. M., Ginley, B. & Sarder, P. Histo-fetch -- On-the-fly processing of gigapixel whole slide images simplifies and speeds neural network training. *arXiv preprint arXiv:2102.11433* (2021).

2 McInnes, L., Healy, J. & Melville, J. Umap: Uniform manifold approximation and projection for dimension reduction. *arXiv preprint arXiv:1802.03426* (2018).

3 Ginley, B. *et al.* Computational segmentation and classification of diabetic glomerulosclerosis. **30**, 1953-1967 (2019).